Theoretical Compton profiles due to valence electrons of Ti and TiH_2

1986 J. Phys. F: Met. Phys. 16 1471

(http://iopscience.iop.org/0305-4608/16/10/014)

J. Phys. F: Met. Phys. **16** (1986) 1471–1483. Printed in Great Britain

Theoretical Compton profiles due to valence electrons of Ti and TiH_2

N C Bacalis†, N I Papanicolaou‡ and D A Papaconstantopoulos§

† Research Centre of Crete, PO Box 1527, Iraklion, Crete GR-711 10, Greece
‡ Department of Physics, University of Ioannina, Ioannina, GR-453 32, Greece
§ Naval Research Laboratory, Washington, DC 20375, USA

Received 29 October 1985

Abstract. We calculate the Compton profiles of Ti and TiH_2, due to their valence electrons, along the [100], [110] and [111] directions, based on self-consistent augmented plane-wave functions. We present the main theoretical points of our method and the Compton profiles of Ti (FCC), Ti (BCC) and TiH_2 (CaF_2 structure), as well as their directional anisotropies. The average Compton profile of Ti (FCC) is in good agreement with available experiments for Ti (HCP). The introduction of hydrogen in forming TiH_2 causes remarkable changes in the Compton profiles.

1. Introduction

There is current interest in studying the electronic properties of metal hydrides, particularly as they concern hydrogen, because of their usefulness in energy storage (Bambakidis 1981). In recent years, measurements of their Compton profiles (CP) have been widely used to understand their electronic structure (Itoh *et al* 1980, Reed 1978, Felsteiner *et al* 1981, Theodoridou and Alexandropoulos 1984). As is the case for other transition metals, Ti easily absorbs large quantities of hydrogen (Alexandropoulos *et al* 1983, Stalinski and Beganski 1962), so one can obtain experimental measurements on the CP of TiH_x, where $x \lesssim 2$. This prompts interest in theoretically calculating the CP of Ti and TiH_2, to see any effects due to the introduction of hydrogen.

Ti crystallises in the HCP structure (α phase) and, for $T > 900\,^{\circ}C$, in the BCC structure (β phase). Its CP has been studied experimentally (Weiss 1972, Manninen and Paakkari 1976, Felsteiner and Pattison 1976) for polycrystalline Ti (HCP) using X-rays or γ rays and its isotropic CP has been calculated in the renormalised free-atom model (RFA) (Berggren *et al* 1977, Krishna Gandhi and Singru 1981). The CP of Ti for the high-temperature (BCC) phase has not been studied. TiH_2 crystallises in the CaF_2 structure with Ti at (0, 0, 0) and H at $(\pm a/4, \pm a/4, \pm a/4)$, and to our knowledge no experimental or theoretical study of its CP exists.

Here we report a calculation of the directional CPs for Ti (FCC), Ti (BCC) and TiH_2 based on the results of augmented plane-wave (APW) band-structure calculations. We believe that the theoretical average CP calculation of Ti (FCC) simulates well the experimentally measured Ti (HCP) CP, because the two structures have the same density. Our results (figure 1) essentially coincide with the experimental results of Manninen and

0305-4608/86/101471 + 13 $02.50

Paakkari (1976) (within the experimental error), indicating that the FCC approximation is reasonable. TiH_2 has different electronic properties from Ti (Papaconstantopoulos and Switendick 1984) that result in the differences in their CPs. Our calculations are from first principles based on APW band-structure wavefunctions.

2. Method of calculation and approximations

The band-structure calculations are performed self-consistently using the symmetrised APW method (SAPW) (Mattheiss *et al* 1968) in the 'soft-core' approximation as described elsewhere (Bacalis *et al* 1985). The mass–velocity and Darwin relativistic corrections (Koelling and Harmon 1977) are included, but spin–orbit coupling is neglected. The exchange and correlation part of the crystal potential is treated in the local density formalism of Hedin and Lundqvist (1971). The core levels of Ti are calculated by a fully relativistic atomic-like calculation for each iteration. The outer levels are calculated self-consistently with the APW method on a mesh of NK points in $\frac{1}{48}$th of the first Brillouin zone (BZ); $N=20$ for the FCC and $N=14$ for the BCC structure. Convergence is assumed when the eigenvalues of two successive iterations agree to within 10^{-4} Ryd.

The lattice constants are taken (in au) as $a=7.7400$ for Ti (FCC), 6.2484 for Ti (BCC) and 8.3904 for TiH_2 (FCC). The muffin-tin (MT) sphere radii in TiH_2 are $R_{Ti}=2.3622$ au and $R_H=1.2718$ au (Papaconstantopoulos and Switendick 1984). The converged crystal potential is used to calculate final APW wavefunctions on a mesh of 89 K points and 55 K points for the FCC and BCC irreducible Brillouin zones, respectively.

The wavefunctions are written (Mattheiss *et al* 1968) as

$$\psi_n(\boldsymbol{K},\boldsymbol{r})=\sum_i v(\boldsymbol{k}_i)\varphi(\boldsymbol{r},\boldsymbol{k}_i,n) \qquad \boldsymbol{k}_i=\boldsymbol{K}+\boldsymbol{G}_i$$

where $\boldsymbol{G}_i$ are reciprocal lattice vectors around the centre of the first BZ (181 for FCC, 87 for BCC), $\boldsymbol{K}$ is a certain K point in the $\frac{1}{48}$th BZ, n is a band index, $v(\boldsymbol{k}_i)$ are eigenvectors from the secular equation whose dimensionality is taken to be 70×70 for Ti and 90×90 for TiH_2, and $\varphi(\boldsymbol{r},\boldsymbol{k}_i,n)$ are APW functions. In an obvious and common notation, for N_A atoms in the unit cell,

$$\varphi(\boldsymbol{r},\boldsymbol{k}_i,n)=\exp(\mathrm{i}\boldsymbol{k}_i\cdot\boldsymbol{r}) \qquad \boldsymbol{r} \text{ outside the MT spheres}$$

$$\varphi(\boldsymbol{r},\boldsymbol{k}_i,n)=\exp(\mathrm{i}\boldsymbol{k}_i\cdot\boldsymbol{r}_{MT})\sum_{l=0}^{\infty}\sum_{m=-l}^{l}(2l+1)\mathrm{i}^l\frac{j_l(k_iR_{MT})}{u_l(R_{MT},n)}$$
$$\times u_l(r,n)\frac{(l-|m|)!}{(l+|m|)!}P_l^m(\cos\theta)P_l^m(\cos\theta_i)$$
$$\times\exp[\mathrm{i}m(\varphi-\varphi_i)] \qquad \boldsymbol{r} \text{ inside the MT spheres, MT}=1,\ldots,N_A.$$

Here $\boldsymbol{r}_{MT}$ is the MT centre, R_{MT} the MT radius, $(r,\theta,\varphi)\equiv\boldsymbol{r}-\boldsymbol{r}_{MT}$, $u_l(r,n)$ are the corresponding radial functions, $j_l(kr)$ are spherical Bessel functions, P_l^m are associated Legendre polynomials and θ_i, φ_i are the spherical coordinates of $\boldsymbol{k}_i$ with respect to a coordinate system centred at $\boldsymbol{r}_{MT}$.

The Fourier transform of $\psi_n(\boldsymbol{K},\boldsymbol{r})$ is equal to

$$\chi_n(\boldsymbol{K},\boldsymbol{p})=\sum_i v(\boldsymbol{k}_i)(\hat{f}^{PW}_{\boldsymbol{p},\boldsymbol{k}_i}+\hat{f}^{IN}_{\boldsymbol{p},\boldsymbol{k}_i}) \qquad \boldsymbol{p}=\boldsymbol{K}+\boldsymbol{G}$$

where $\boldsymbol{G}$ in practice belongs to the set $\{\boldsymbol{G}_i\}$,

$$\hat{f}^{\mathrm{PW}}_{\boldsymbol{p},\boldsymbol{k}_i} = \left(V_{\mathrm{cell}} - \sum_{\mathrm{MT}=1}^{N_{\mathrm{A}}} V_{\mathrm{MT}}\right)\delta_{\boldsymbol{p},\boldsymbol{k}_i} - 4\pi \sum_{\mathrm{MT}=1}^{N_{\mathrm{A}}} (1-\delta_{\boldsymbol{P},\boldsymbol{k}_i}) \times \exp[\mathrm{i}(\boldsymbol{k}_i-\boldsymbol{P})\cdot\boldsymbol{r}_{\mathrm{MT}}] R^2_{\mathrm{MT}} \frac{j_1(|\boldsymbol{k}_i-\boldsymbol{p}|R_{\mathrm{MT}})}{|\boldsymbol{k}_i-\boldsymbol{P}|}$$

with V_{cell} the volume of unit cell and V_{MT} the volume of each MT sphere, and

$$\hat{f}^{\mathrm{IN}}_{\boldsymbol{p},\boldsymbol{k}_i} = 4\pi \sum_{\mathrm{MT}=1}^{N_{\mathrm{A}}} \exp(\mathrm{i}\boldsymbol{k}_i\cdot\boldsymbol{r}_{\mathrm{MT}}) \sum_{l=0}^{3} \frac{j_l(k_i R_{\mathrm{MT}})}{u_l(R_{\mathrm{MT}},n)}(2l+1) \times P_l\left(\frac{\boldsymbol{p}\cdot\boldsymbol{k}_i}{|\boldsymbol{p}|\,|\boldsymbol{k}_i|}\right) \int_0^{R_{\mathrm{MT}}} r^2 u_l(r,n) j_l(pr)\,\mathrm{d}r.$$

For each $\boldsymbol{K}$, the normalisation condition is $\Sigma_{\boldsymbol{G}}|\chi_n(\boldsymbol{K},\boldsymbol{p})|^2 = 1$.

The electron momentum distribution is obtained from

$$n(\boldsymbol{p}) = \sum_{n\ \mathrm{occupied}} \sum_{\boldsymbol{K}}^{\mathrm{BZ}} \sum_{\boldsymbol{G}} \delta_{\boldsymbol{p},\boldsymbol{K}+\boldsymbol{G}} \frac{1}{N} |\chi_n(\boldsymbol{K},\boldsymbol{p})|^2 = \sum_{\boldsymbol{K}}^{\frac{1}{48}\mathrm{BZ}} \sum_{\boldsymbol{G}} \delta_{\boldsymbol{p},\boldsymbol{K}+\boldsymbol{G}} \frac{1}{N} |\chi_n(\boldsymbol{K},\boldsymbol{p})|^2 \frac{w(\boldsymbol{K})}{T}$$

where N is a normalisation constant, $w(\boldsymbol{K})$ is the weight of $\boldsymbol{K}$ in the $\frac{1}{48}$th BZ ($=0$ if $E(\boldsymbol{K}) > E_{\mathrm{Fermi}}$) and $T = \Sigma_{\boldsymbol{K}} w(\boldsymbol{K})$.

The CP due to the outer electrons (in the impulse approximation) (Platzman and Tzoar 1965, Eisenberger and Platzman 1970) in a direction $\hat{\boldsymbol{e}}$ for a momentum $q = q\hat{\boldsymbol{e}}$ is given by

$$J(q,\hat{\boldsymbol{e}}) = \sum_{\boldsymbol{p}} n(\boldsymbol{p})\delta(\boldsymbol{p}\cdot\hat{\boldsymbol{e}} - q) = \sum_{\boldsymbol{p}} \sum_{\boldsymbol{K}}^{\frac{1}{48}\mathrm{BZ}} \sum_{\boldsymbol{G}} \sum_{\alpha} \delta_{\boldsymbol{p},\boldsymbol{K}+\boldsymbol{G}} \frac{1}{N} |\chi_n(\boldsymbol{K},\boldsymbol{p})|^2 \frac{w(\boldsymbol{K})}{T} \delta(\boldsymbol{p}\cdot(\alpha\hat{\boldsymbol{e}}) - q)$$

where the set of $\{\alpha\hat{\boldsymbol{e}}\}$ is the star of $\hat{\boldsymbol{e}}$ for the point group of $\boldsymbol{K}$ (Rath *et al* 1973). The symmetry operator appears inside the δ function.

The normalisation of CP for each $\hat{\boldsymbol{e}}$ should be satisfied: $\int_{-\infty}^{\infty} J(q,\hat{\boldsymbol{e}})\,\mathrm{d}q =$ number of outer electrons per unit cell (4 for Ti and 6 for TiH_2).

We calculated the CPs for three $\hat{\boldsymbol{e}}$ directions: [100], [110] and [111]. The average CP was computed from

$$J_{\mathrm{ave}} = (1/26)(6J_{100} + 12J_{110} + 8J_{111}).$$

To check the convergence of our calculations we performed a calculation of the CP for Ti (BCC) with 285 K points in the $\frac{1}{48}$th BZ (instead of 55), as well as another one with $l_{\max} = 5$ instead of $l_{\max} = 3$. The results, for $q = 0$, showed maximum differences of 1% and 0.2% for the K point and l-convergence tests, respectively.

3. Results and discussion

The results in figures 2–4 and 6–7 show the CPs and the Compton anisotropies, respectively, for the three directions mentioned in § 2. A cubic spline interpolation has been

Table 1. Experimental and theoretical Compton profiles of titanium: (1), Manninen and Paakkari (1976); (2), Felsteiner and Pattison (1976); (3), Weiss (1972); (4) Krishna Gandhi and Singru (1981).

q	$J(q)$					
(au)	Expt (1)	Expt (2)	Expt (3)	RFA (1)	RFA (4)	Present theory (FCC)
0.0	5.500 ± 0.06	5.508 ± 0.09	5.51 ± 0.15	5.551	5.496	5.491
0.1	5.475	5.494		5.521	5.467	5.500
0.2	5.385	5.375	5.40	5.428	5.384	5.438
0.3	5.232	5.177		5.275	5.248	5.256
0.4	5.026	5.022	5.19	5.057	5.047	5.042
0.5	4.777	4.725		4.772	4.785	4.753
0.6	4.498	4.491	4.76	4.420	4.470	4.480
0.7	4.205	4.131		4.001	4.086	4.220
0.8	3.908	3.854	3.92	3.544	3.641	4.008
0.9	3.617	3.501		3.380		3.690
1.0	3.340 ± 0.06	3.211 ± 0.07	3.22	3.202	3.166	3.355
1.1	3.078	2.971		3.016		3.041
1.2	2.836	2.858	2.66	2.824	2.797	2.777
1.3	2.613	2.628		2.638		2.553
1.4	2.410	2.383	2.36	2.446	2.428	2.365
1.5	2.225	2.162		2.263		2.201
1.6	2.056	1.982	2.04	2.092	2.088	2.038
1.7	1.902	1.905		1.931		1.896
1.8	1.763	1.751	1.73	1.782	1.786	1.760
1.9	1.635	1.666		1.645		1.627
2.0	1.520 ± 0.03	1.523	1.51 ± 0.10	1.523	1.529	1.491
2.2	1.322	1.349		1.317		1.269
2.4	1.168	1.153	1.17	1.156	1.162	1.135
2.6	1.049	1.062		1.028		1.021
2.8	0.946	0.957	0.98	0.925		0.907
3.0	0.852 ± 0.02	0.862 ± 0.05		0.844	0.848	0.819
3.5	0.679	0.736		0.701		0.676
4.0	0.581 ± 0.02	0.592	0.59	0.600		0.580
4.5	0.474					0.502
5.0	0.423	0.423	0.46	0.449	0.448	0.438
6.0	0.314	0.321	0.36	0.336		0.331
7.0	0.235 ± 0.01	0.252 ± 0.02	0.27 ± 0.02	0.251		0.249

performed on the CPs to compare with experiments and calculate the anisotropies. Both experimental and theoretical Compton profiles for titanium are listed in table 1 (see also Berggren *et al* 1977) along with the present self-consistent calculation, and are shown in figure 1. The total average CP of Ti, as well as of TiH_2, is obtained by taking the average CP (J_{ave}) for their valence electrons and adding it to a Ti core ($1s^2 2s^2 2p^6 3s^2 3p^6$) atomic CP, calculated by Biggs *et al* (1975). (The total CP of TiH_2 is not shown in table 1.) The outer electron configuration for Ti in the RFA model is taken to be $3d^2 4s^2$ (Manninen and Paakkari 1976, Krishna Gandhi and Singru 1981), while our APW calculations give an electron distribution of $d^{2.9}$ and $(s + p)^{1.1}$. Our results agree well with experiments and are generally within the experimental errors.

Figure 1 shows the calculated total average CP for Ti (FCC) along with the experimental CP for polycrystalline Ti (HCP) of Manninen and Paakkari (1976). The remarkable coincidence of this curve with the data points indicates that the FCC calculation (due to the

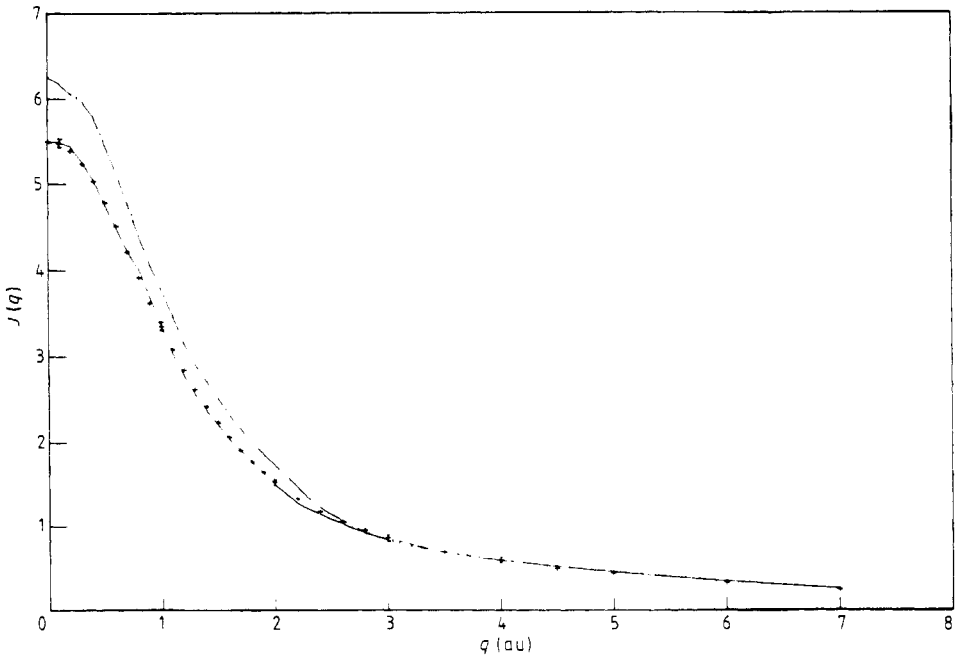

Figure 1. The total average Compton profile, $J(q)$, of Ti (FCC) (full curve) and TiH_2 (dotted curve). The experimental points are taken from Manninen and Paakkari (1976).

same close packing of FCC and HCP) simulates the HCP structure reasonably well. In the same figure we show the total average CP of TiH_2 for comparison with that of Ti. Figures 2, 3 and 4 show the calculated directional CPs due to the valence electrons of Ti (FCC and BCC) and TiH_2, along the [100], [110] and [111] directions, respectively. The local wiggles seem to follow the general interpretations of Wakoh and Yamashita (1973) and Wakoh *et al* (1976) and Rollason *et al* (1983). The band structures of Ti (FCC), Ti (BCC) and TiH_2 are shown in figures 5(*a*), (*b*) and (*c*), respectively. One can see from these figures that the introduction of hydrogen 'pulls' states at the two low-energy bands. The lowest band represents hydrogen–metal bonding states, corresponding to the first band of the host metal. The other band is due to the H–H and H–Ti interactions. The Γ_2' level (antibonding states) lies above the Fermi level as well as above the d states at Γ_{25}'. Our figure 5(*c*) shows small differences from figure 1 of Papaconstantopoulos and Switendick (1984) in the position of the states Γ_1 and Γ_2' with respect to E_F due to an error in the plotting of the energy bands in that paper. However, the topology of the Fermi surface remains the same.

The Fermi level cuts the conduction bands (thus introducing hole states) in the ranges (0.20–0.47) of ΓX, (0.23–0.69) of ΓL and (0.22–0.41) of ΓK, which seem to be reflected in the repeated zone scheme in the CPs of TiH_2 as wiggles. These are convex in the [111] direction and concave in the [100] and [110] directions. At the edges of the BZ there are also local maxima or minima. The general shapes of the CPs for Ti (FCC) and TiH_2 resemble each other the most for the [100] direction and the least for the [111] direction. This is due to the introduction of hydrogen in the [111] direction (at $(\pm a/4, \pm a/4, \pm a/4)$) which affects the charge distribution, and consequently the electron momentum distribution, mainly along the [111] direction, and to lesser extent along the [100] direction.

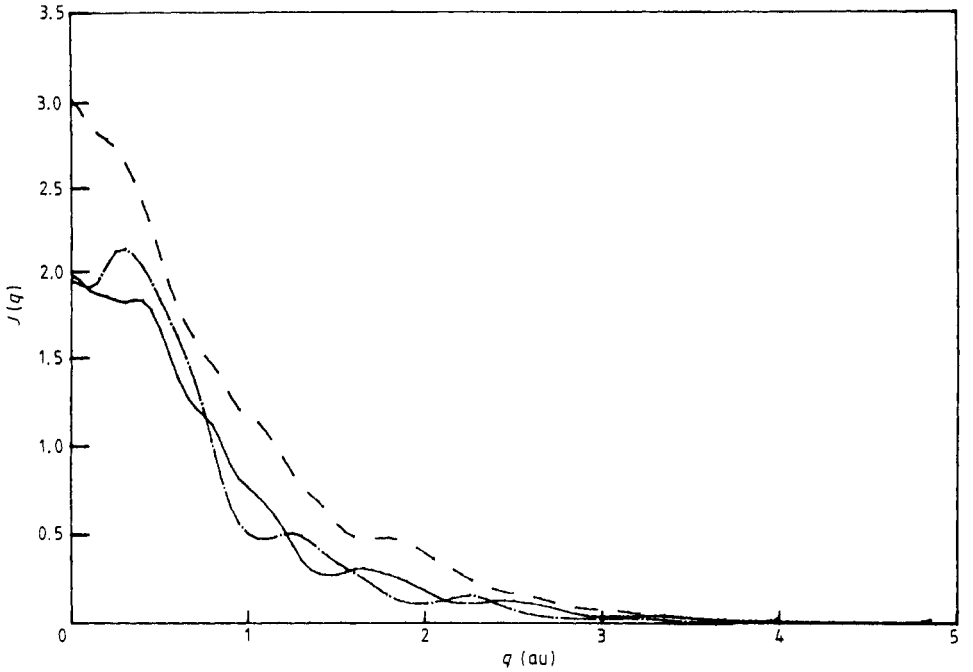

Figure 2. The theoretical directional Compton profiles for the valence electrons along the [100] direction. Full curve, Ti (FCC); dotted curve, Ti (BCC); broken curve, TiH_2.

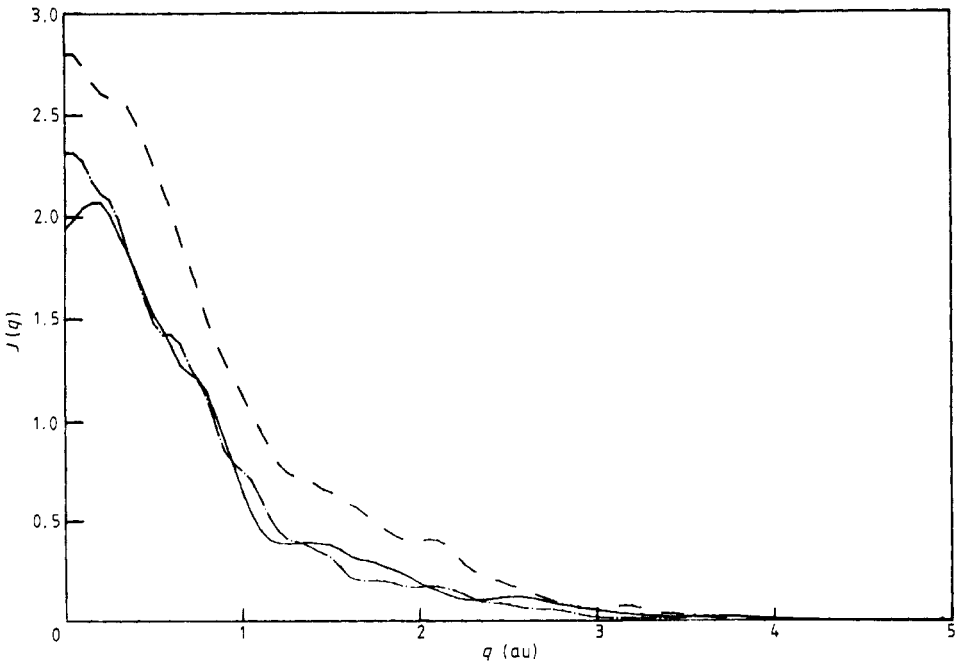

Figure 3. As figure 2, but along the [110] direction.

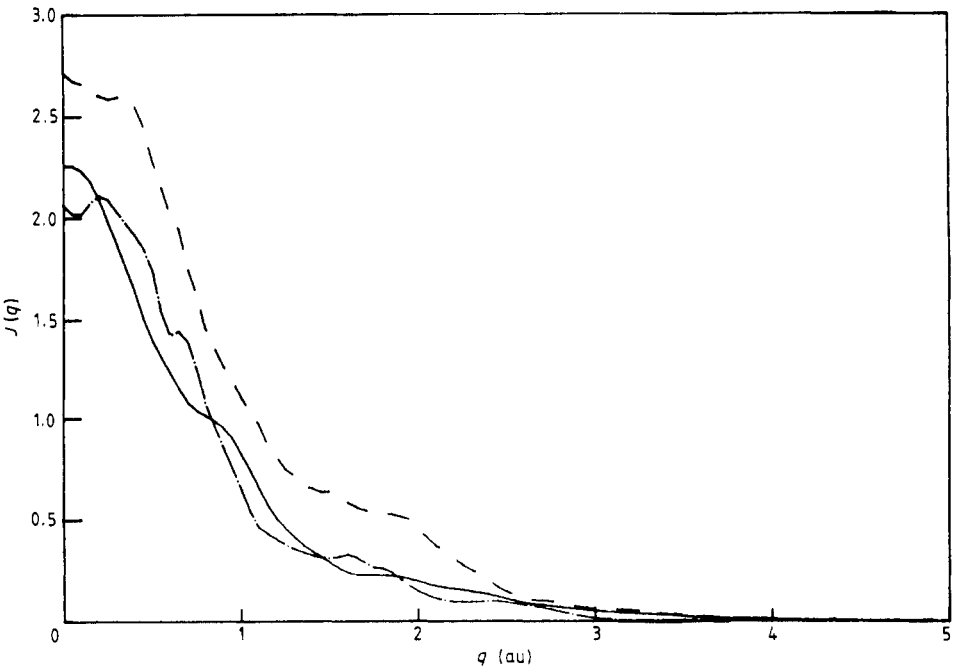

Figure 4. As figure 2, but along the [111] direction.

The periodicity which reveals some information about the projection of the electron or hole states constituting the Fermi surface is shown in the figures for the CPs of Ti and TiH_2 and is described below. With a period $T=2\pi/a$, $2\pi\sqrt{2}/a$, and $2\pi\sqrt{3}/a$ for the directions [100], [110] and [111] respectively, there are repeated wiggles mainly at $q\simeq(n+\delta_i)T/2$ where $n=0, 1, 2, \ldots$ and $\delta_1=0$, $\delta_2=0.13$, $\delta_3=0.44$ and $\delta_4=0.63$. At these positions the wiggles are either convex (+) or concave (−) and their sign shows some periodic pattern. For example, the [100] CP of Ti shows some bumps at $q=nT/2$, whereas in the same CP of TiH_2 there are bumps at $q=(n+\frac{1}{2})T$ and dips at $q=nT$. In the [111] direction for Ti there are only dips at $q=nT$ and for TiH_2 there are bumps at $q=(n+\frac{1}{2})T$ and dips at $q=nT$. In the [110] direction the reverse happens: there are only bumps for TiH_2 whereas bumps interchange with dips for Ti. Thus we can see in more detail how the introduction of H in the FCC structure affects the directional CPs.

The differences in the order of concaves of the [100] and [110] CPs between Ti to TiH_2 are mainly due to the difference in their band structures. For small q the CPs of Ti and TiH_2 in the [100] direction are similar, whereas they are very different in the [111] direction. In Ti the [111] CP looks like a free-electron gas CP, whereas in TiH_2 it shows a significant structure (quite similar to the [100] CP of Ti). This difference is due evidently to the presence of hydrogen in the [111] directions, which introduces deep bonding orbitals (Papaconstantopoulos and Switendick 1984) along these directions, and the momentum density is less likely to be directed along the bonds (Epstein and Tanner 1977). Something similar but less pronounced happens in the [110] direction in going from Ti to TiH_2. In order to check these results we calculated the CPs of TiH_2 with 20 K points in the $\frac{1}{48}$th first BZ. Although the absolute values differ slightly from the 89 K-point mesh, the main features are preserved.

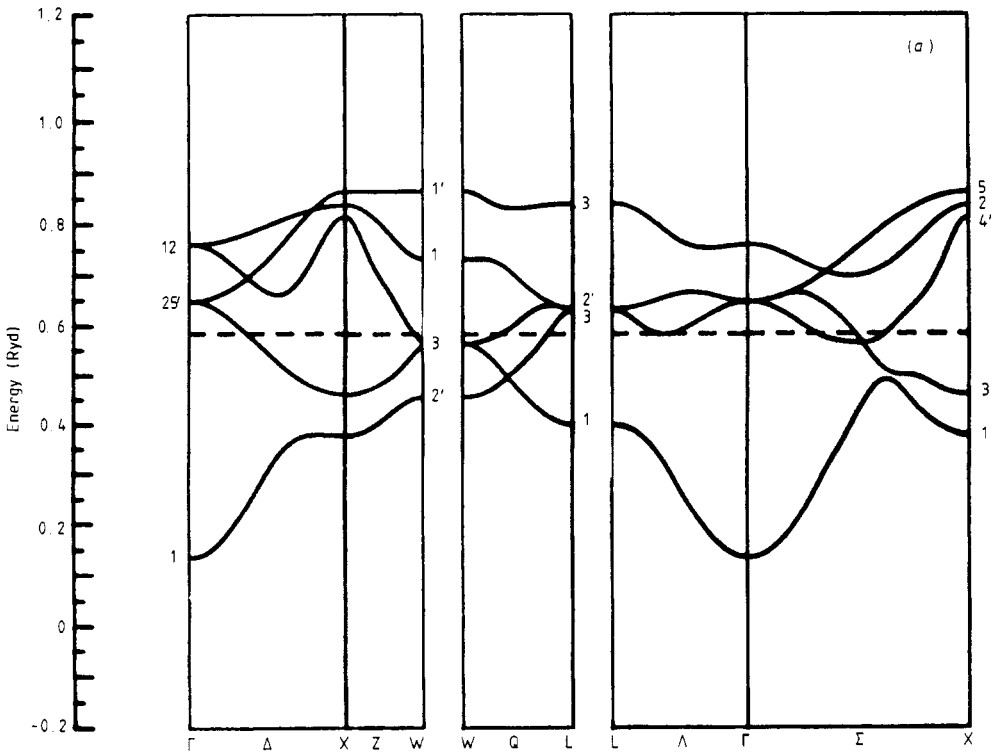
(a)
Energy (Ryd)
1.2
1.0
0.8
0.6
0.4
0.2
0
-0.2
Γ Δ X Z W
W Q L
L Λ Γ Σ X

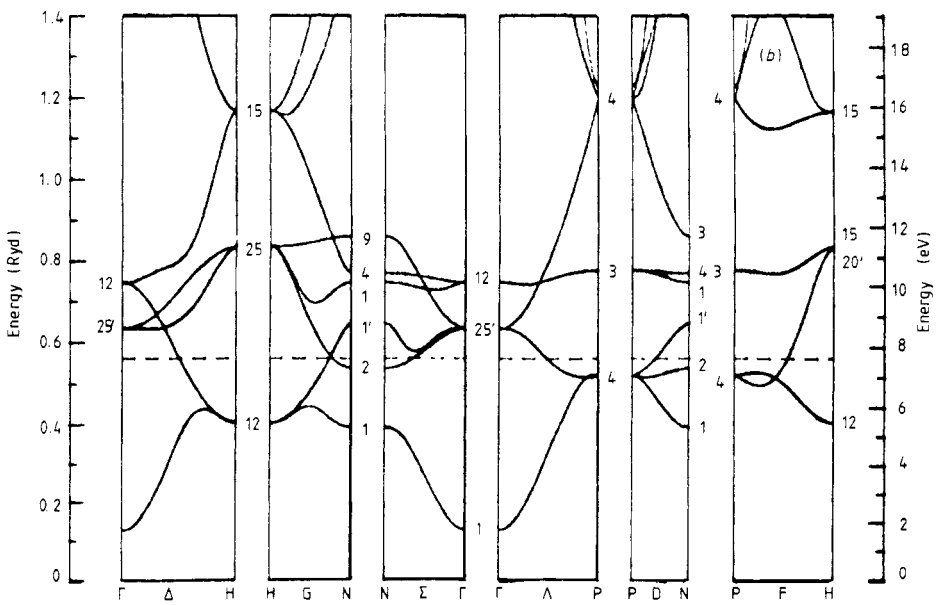
(b)
Energy (Ryd)
Energy (eV)
Γ Δ H
H G N
N Σ Γ
Γ Λ P
P D N
P F H

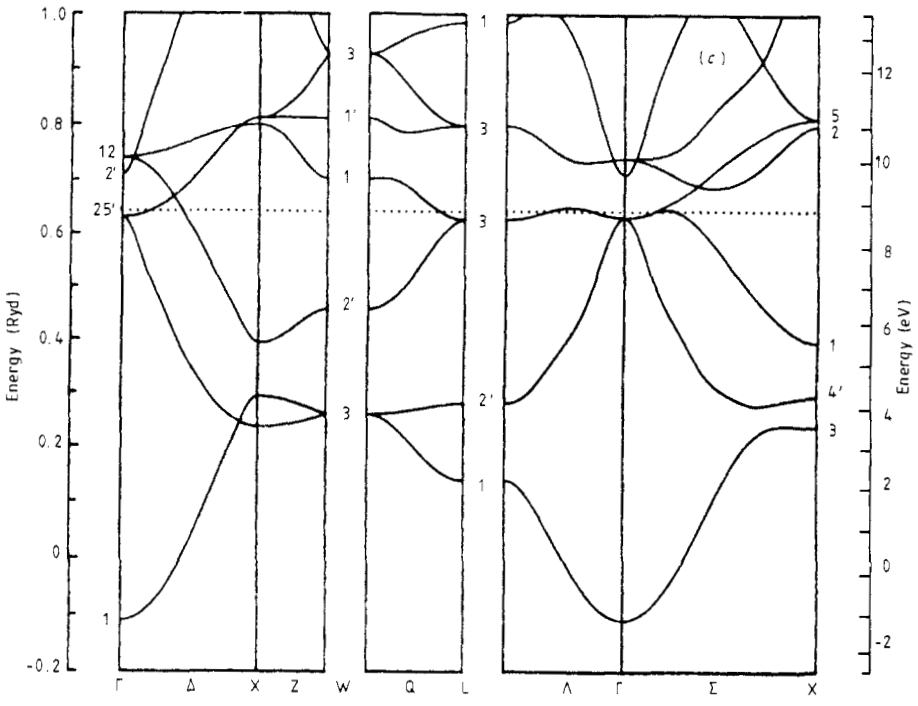

Figure 5. Energy bands of (*a*) Ti (FCC), (*b*) Ti (BCC) and (*c*) TiH_2.

Similar observations can be made for the CPs of Ti (BCC). For large q they are periodically convex and concave with periods again equal to $2\pi/a$, $2\pi\sqrt{2}/a$ and $2\pi\sqrt{3}/a$ for each direction examined. The [100] CP is concave at $q=nT/2$ and convex at $q=(n+\frac{1}{2})T/2$. The [110] CP is convex at $q=nT/4$ and the [111] CP is roughly convex at $q=nT/2$ and concave at $q=(n+\frac{1}{2})T/4$. For small q the most similar to the free-electron gas CP is in the [110] direction, the most different in the [100] and the [111] CP is in between. In both the FCC and BCC structures, the direction which is less dense in atoms ([111] for FCC and [110] for BCC), has a CP similar to the free-electron gas for small q (long wavelengths).

Figures 6(*a*), (*b*) and (*c*) show the directional anisotropies in the CPs for both FCC and BCC Ti: figure 6(*a*) shows $J_{111}-J_{100}$, figure 6(*b*) shows $J_{111}-J_{110}$ and figure 6(*c*) shows $J_{110}-J_{100}$. Figures 7(*a*), (*b*) and (*c*) show the corresponding differences for TiH_2. Evidently there are remarkable anisotropies. The most interesting feature, we think, is that the anisotropies for Ti (BCC and FCC), between the [111] and the [110] directions, (i.e. between the most and least dense directions in each structure), are essentially opposite in sign. In other words the anisotropies ($J_{\text{most dense}}-J_{\text{least dense}}$) for the two structures agree in sign for almost all values of q. Generally the anisotropies follow a normal pattern resembling roughly the shape of a function like $(\sin x)/x$. The anisotropy that diverges the most from this pattern is the $J_{111}-J_{110}$ for both TiH_2 and Ti (BCC) (i.e. between the two most dense directions in both structures). These are roughly similar to each other but the one of Ti (BCC) is more pronounced. Thus we can say that the anisotropies are governed significantly by the densities in atoms of the various directions (in real space).

Figure 8 shows the difference between the average CPs of TiH_2 and Ti (FCC), along with a CP of atomic hydrogen. They are far from similar. However, it is believed

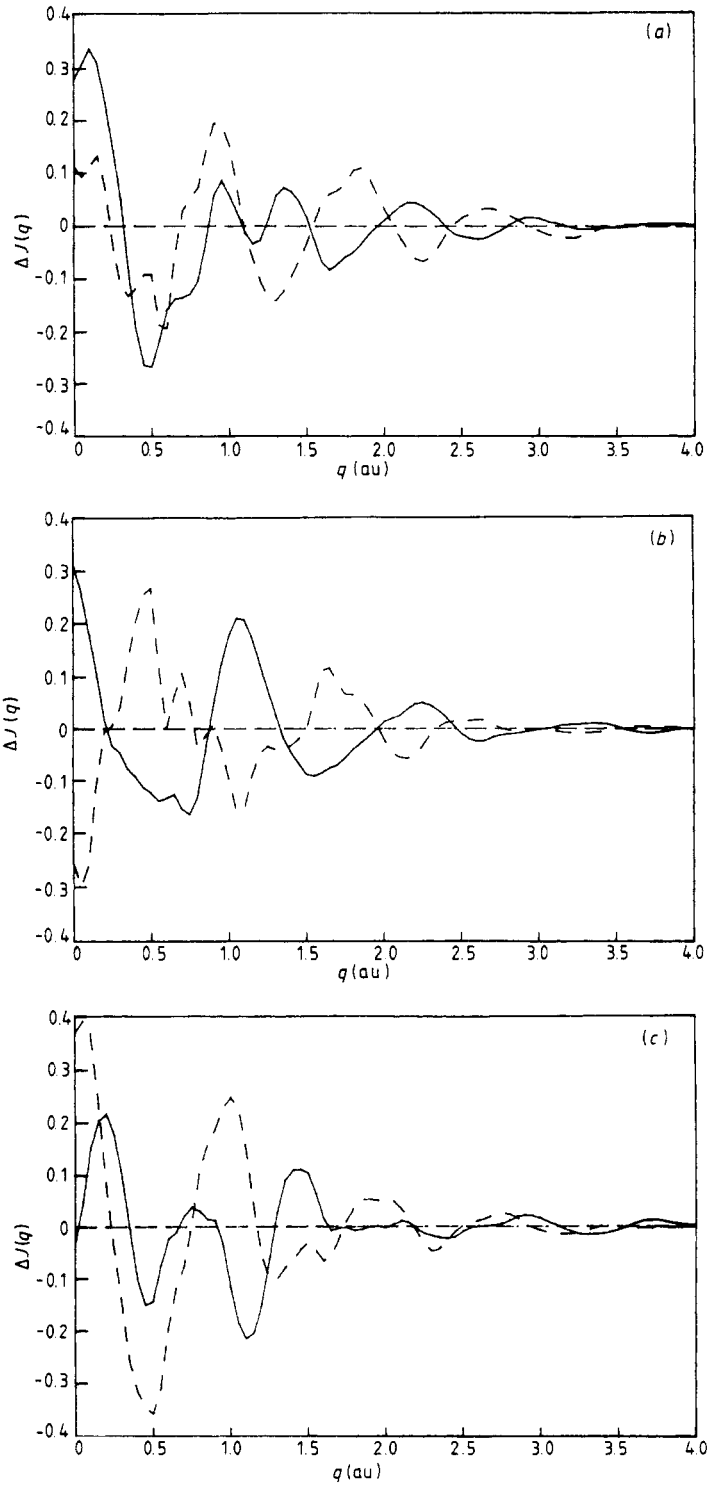

Figure 6. Anisotropy in the theoretical Compton profiles of Ti: (*a*) $J_{111}-J_{100}$, (*b*) $J_{111}-J_{110}$ and (*c*) $J_{110}-J_{100}$ (full curve, Ti (FCC); broken curve, Ti (BCC).

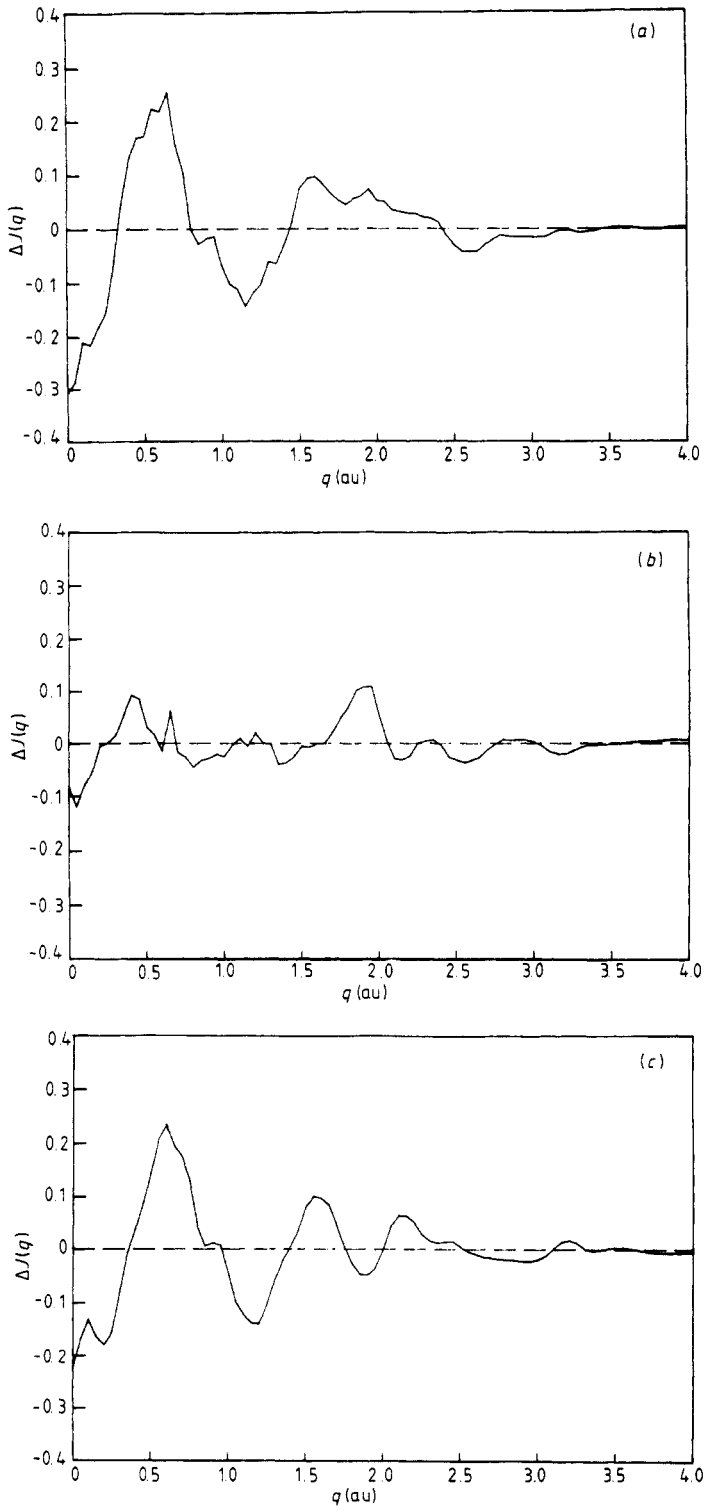

Figure 7. Theoretical anisotropies for TiH_2: (*a*) $J_{111}-J_{100}$, (*b*) $J_{111}-J_{110}$ and (*c*) $J_{110}-J_{100}$.

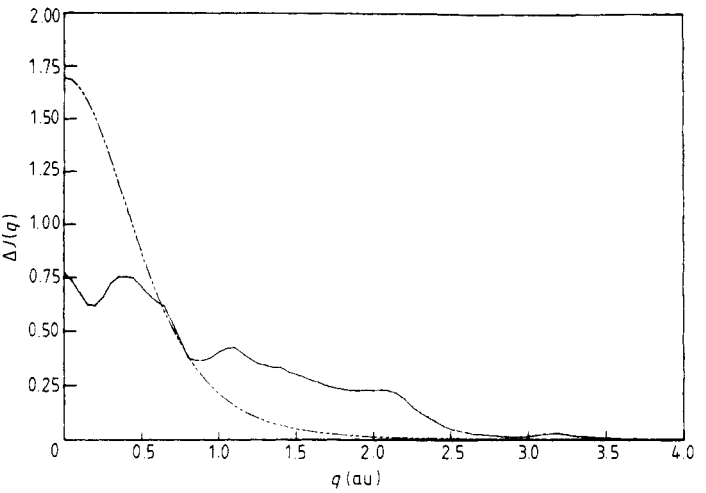

Figure 8. Difference, $\Delta J(q)$, between the theoretical average Compton profiles of TiH_2 and Ti (FCC) (full curve) compared with the theoretical Compton profile of atomic hydrogen (broken curve).

(Theodoridou and Alexandropoulos 1984, Alexandropoulos *et al* 1983) that at high concentrations a large amount of hydrogen enters the host metal in atomic form. If this is true, the proposed model by Alexandropoulos *et al* (1983) of trapping the hydrogen among the grains would be supported.

Finally let us make the following observation concerning the difference between the 'scaled' average CPs of TiH_2 and Ti (FCC), as described below: for each direction $[hkl]$ take $T=(\pi/a)(h^2+k^2+l^2)^{1/2}$, find $J_{hkl}(q/T)$ and define

$$J_{ave}(q/T)=(1/26)(6J_{100}(q/T)+12J_{110}(q/T)+8J_{111}(q/T)).$$

Then the difference $J_{ave}(q/T)_{TiH_2}-J_{ave}(q/T)_{Ti(FCC)}$ has maxima at $q/T=1, 2, 3, \ldots$.

4. Summary and conclusions

The Compton profiles of Ti (FCC), Ti (BCC) and TiH_2 were calculated with APW wavefunctions, along the [100], [110] and [111] directions. Ti (FCC) simulates well the experimental CP of Ti (HCP). For small q, $J_{hkl}(q)$ resembles the CP of a free-electron gas, for the directions which are less dense in atoms. The most dense directions show significant structure in their CPs for small q. For large q, the wiggles in the CPs show a periodicity with period $(2\pi/a)(h^2+k^2+l^2)^{1/2}$. The CP anisotropies between the above directions seem to be governed by the densities of these directions. Generally $(J_{dense}-J_{dilute})$ follow a canonical pattern whereas $(J_{dense}-J_{dense'})$ is more rough and irregular.

Acknowledgments

We would like to thank Professor N G Alexandropoulos for suggesting these calculations and for valuable discussions, and Dr A C Switendick for discussions on the band theory of

metal hydrides. We would also like to thank Mr K Blathras for kindly performing the calculations with his computer program. One of us (NIP) would like to thank the Research Center of Crete for their hospitality and the use of facilities during this work.

References

Alexandropoulos N G, Boulakis G G, Papadimitriou D and Theodoridou I 1983 *Phys. Status Solidi* b **120** K19

Bacalis N C, Blathras K, Thomaides P and Papaconstantopoulos D A 1985 *Phys. Rev.* B **32** 4849

Bambakidis G (ed.) 1981 *Metal Hydrides* (New York: Plenum)

Berggren K-F, Manninen S, Paakkari T, Aikala O and Mansikka K 1977 *Compton Scattering* ed. B Williams (New York: McGraw-Hill) pp 139, 160

Biggs F, Mendelsohn L B and Mann J B 1975 *Atomic Data and Nuclear Data Tables* **16** 201

Eisenberger P and Platzman P M 1970 *Phys. Rev.* A **2** 415

Epstein I R and Tanner A C 1977 *Compton Scattering* ed. B Williams (New York: McGraw-Hill) p 217

Felsteiner J, Heilper M, Gertner I, Tanner A C, Opher R and Berggren K F 1981 *Phys. Rev.* B **23** 5156

Felsteiner J and Pattison P 1976 *Phys. Rev.* B **13** 2702

Hedin L and Lundqvist B I 1971 *J. Phys. C: Solid State Phys.* **4** 2064

Itoh F, Honda T, Asano H, Hirabayashi M and Suzuki K 1980 *J. Phys. Soc. Japan* **49** 202 and references therein

Koelling D D and Harmon B N 1977 *J. Phys. C: Solid State Phys.* **10** 3107

Krishna Gandhi K R and Singru R M 1981 *Phil. Mag.* B **43** 999

Manninen S and Paakkari T 1976 *J. Phys. C: Solid State Phys.* **9** 95

Mattheiss L F, Wood J H and Switendick A C 1968 *Methods Comput. Phys.* **8** 63

Papaconstantopoulos D A and Switendick A C 1984 *J. Less-Common Met.* **103** 317

Platzman P M and Tzoar N 1965 *Phys. Rev.* **139** A410

Rath J, Wang C S, Tawil R A and Callaway J 1973 *Phys. Rev.* B **8** 5139

Reed W A 1978 *Phys. Rev.* B **18** 1986

Rollason A J, Holt R S and Cooper M J 1983 *Phil. Mag.* B **47** 51

Stalinski B and Beganski Z 1962 *Bull. Acad. Pol. Sci. Ser. Chim.* **10** 247

Theodoridou I and Alexandropoulos N G 1984 *Z. Phys.* B **54** 225

Wakoh S, Kubo Y and Yamashita J 1976 *J. Phys. Soc. Japan* **40** 1043

Wakoh S and Yamashita J 1973 *J. Phys. Soc. Japan* **35** 1406

Weiss R J 1972 *Phil. Mag.* **25** 1511